Quasi-P_1^0 Electromagnetic Response Estimates from Ørsted Vector Data: A Study in Ring Current Asymmetry

Nic Richmond (nic@ucsd.edu), Cathy Constable, Steve Constable and Joseph Ribaudo
IGPP, Scripps Institution of Oceanography, University of California, San Diego, Ca

1. INTRODUCTION

- Electrical conductivity profiles for the Earth can be derived by studying currents induced within the Earth by external time varying magnetic fields of ionospheric or magnetospheric origin
- Many studies have used observatory data, but it has been shown (e.g. Dolginov, 1972; Olsen 1999) that satellite data can also be used to estimate Earth conductivity, by looking at the external and internal fields associated with the time varying magnetospheric currents (see Figure 1)

Figure 1. The toroidal ring current, which circles the Earth at 2-9 Earth radii. It is variable in time and is asymmetric due to the nightside partial ring current. It is the main source current in satellite induction studies.

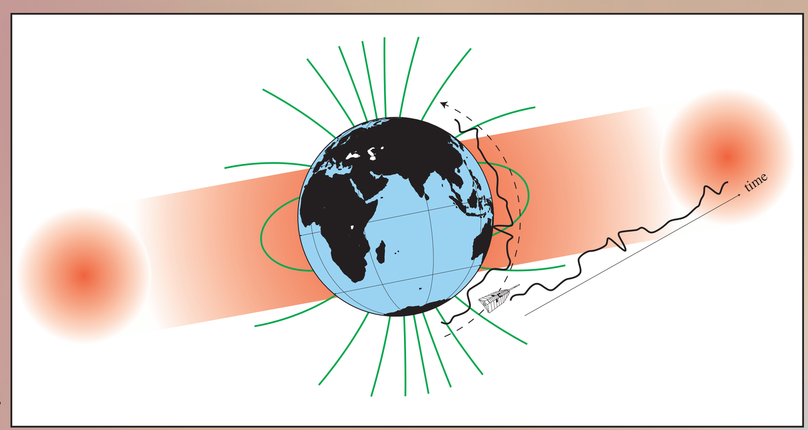

- Using the 7-month Magsat dataset, Constable and Constable (2004) found evidence for a conductivity jump at ~1,300 km depth
- However, because the depth that can be sampled is dependent on the length of the time series available it is uncertain whether that feature is real
- Here, we report results from a study of ~4 years of data from the Ørsted satellite

2. DATA PROCESSING

- Ørsted vector magnetometer data from Nov 2000-Dec 2004
- Need to isolate the currents associated with the magnetospheric ring current (Figure 1) and the associated induced currents
- CHAOS (Olsen et al., 2006) used to correct for the core field and secular variation
- CM4 (Sabaka et al., 2004) used to correct for the lithospheric, ionospheric, constant magnetospheric and toroidal fields

3. ESTIMATING e AND i FOR P_1^0

- The ring current has predominantly P_1^0 structure at mid-latitudes:

$$\Phi_1^0(r,\theta) = a_0\left\{ i_1^o(t)\left(\frac{a_0}{r}\right)^2 + e_1^o(t)\left(\frac{r}{a_0}\right)\right\} P_1^0(\cos\theta)$$

- The magnetic induction B is derived from the negative of the gradient, which is given by the following (as components of a spherical coordinate system):

$$B_r = \left[-e_1^0 + 2i_1^0\left(\frac{a}{r}\right)^3\right]\cos(\theta)$$

$$B_\theta = \left[e_1^0 + i_1^0\left(\frac{a}{r}\right)^3\right]\sin(\theta)$$

$$B_\phi = 0$$

- For each satellite pass, e and i were estimated by an overdetermined least squares approach
- i is approximately 1/3 e, consistent with results from previous studies (e.g. Langel and Estes, 1985; Constable and Constable, 2004)

4. COMPARING SATDST AND SYM-H

- SatDst = e + i
- Figure 2 compares SatDst with pass-averaged SYM-H as a function of local time
- Between ~2am and 10am SatDst gives slightly smaller negative values than SYM-H and the difference is larger, the more negative SYM-H
- Between ~2pm and 10pm SatDst gives larger negative values than SYM-H and again the difference is larger, the more negative SYM-H
- Indicates that we are observing asymmetry in the source field

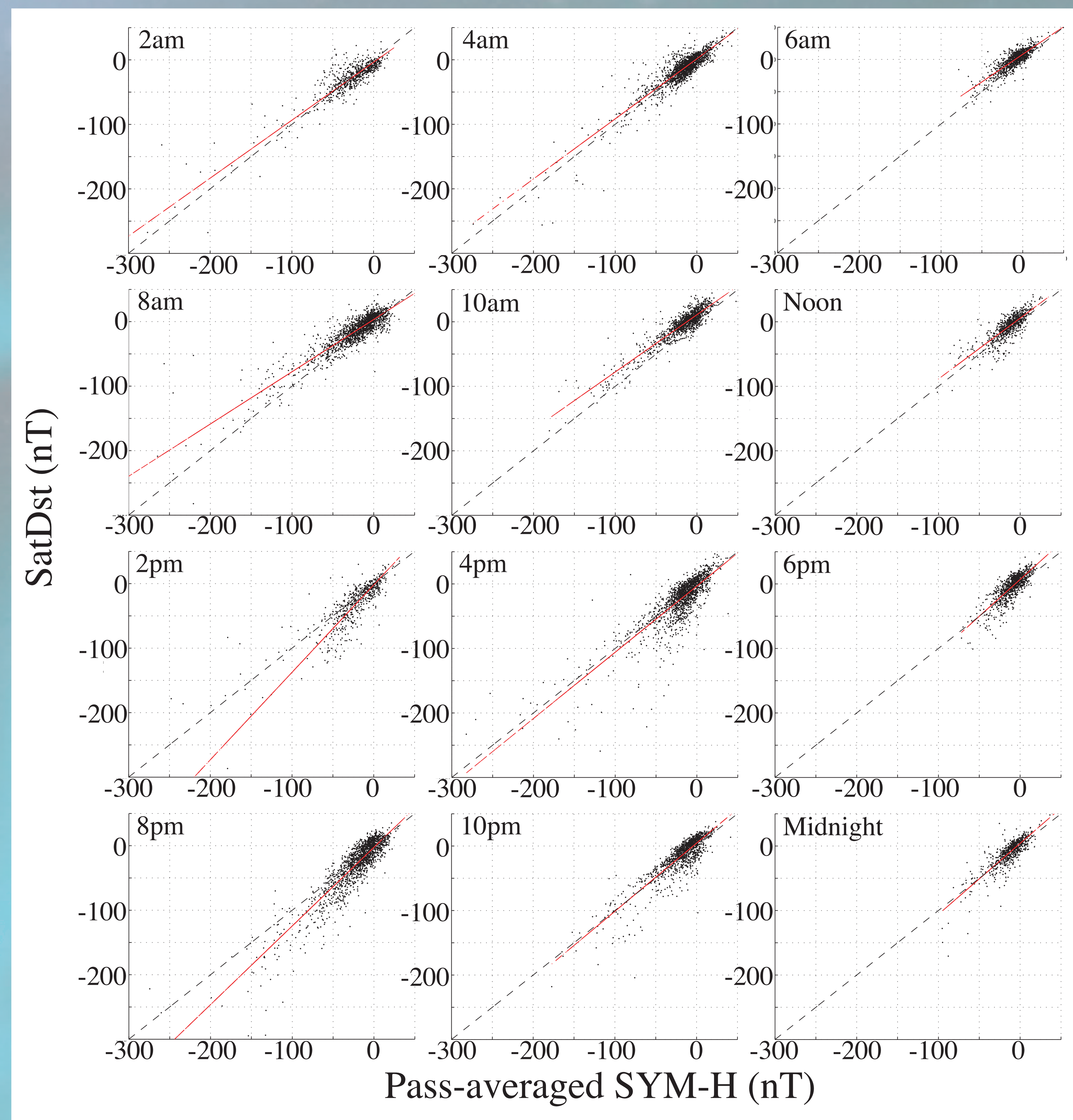

Figure 2. Scatterplots of SatDst against pass-averaged SYM-H for example hourly local time bins. Times give the end time for each hourly bin. The black dotted line shows a 1 to 1 relationship. The red lines are the best fit lines to the data.

5. CAUSES OF THE ASYMMETRY

- One of the main causes is likely to be the partial ring current
- This current results from particles being injected into the inner magnetosphere from the geomagnetic tail during magnetic storms
- The injected particles drift westwards through dusk before closing via the magnetopause or auroral currents at local times close to noon
- This would result in a stronger external field between noon and midnight (via dusk), and a weaker external field during the hours near dawn
- The results in Figure 2 are consistent with this

6. LONG PERIOD CHANGES TO THE ASYMMETRY?

- Figure 3 presents the gradient of the best fit lines between SatDst and pass-averaged SYM-H as a function of local time
- The best fit lines have been determined for each year of data, not for the compilation of years shown in Figure 2

Figure 3. Gradient of the best fit line as a function of local time and year:
x 2001
+ 2002
o 2003
* 2004
· 2005

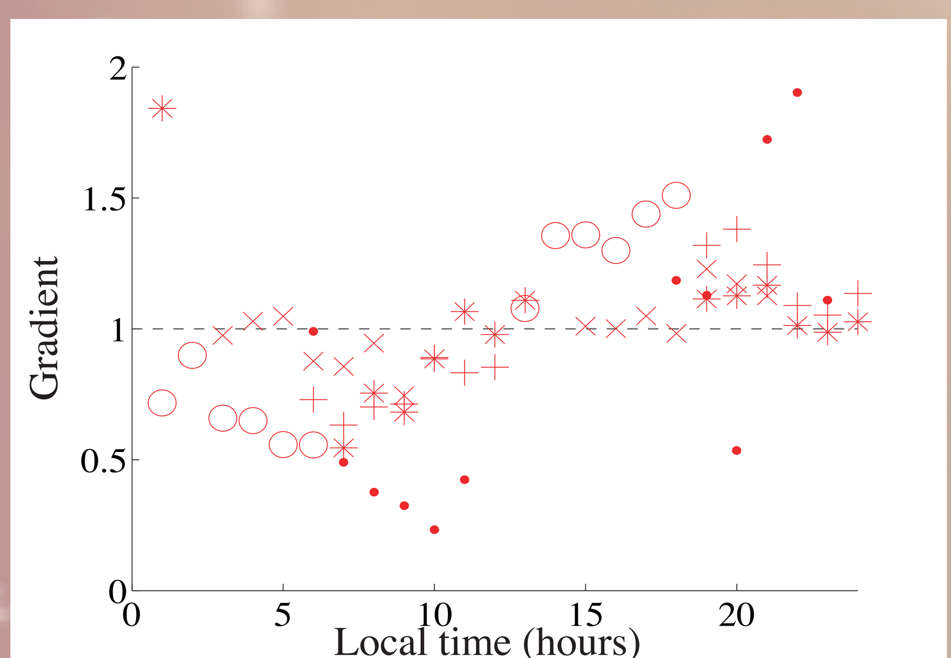

- The gradient is steeper for some years than others (for example 2001 and 2003 for local times between 3 and 6 hours) indicating that the difference between SatDst and pass-averaged SYM-H is larger in some years than others

7. LOCAL TIME EFFECTS ON RESPONSE FUNCTION ESTIMATES

- Figure 4 presents the real and imaginary parts of the C-response for different local time bins from 2001-2003
- Nightside data give values close to those of Balasis et al., 2004
- Dayside values, particularly for the real component, are quite different to the nightside data
- This difference is due to local time effects in the source current

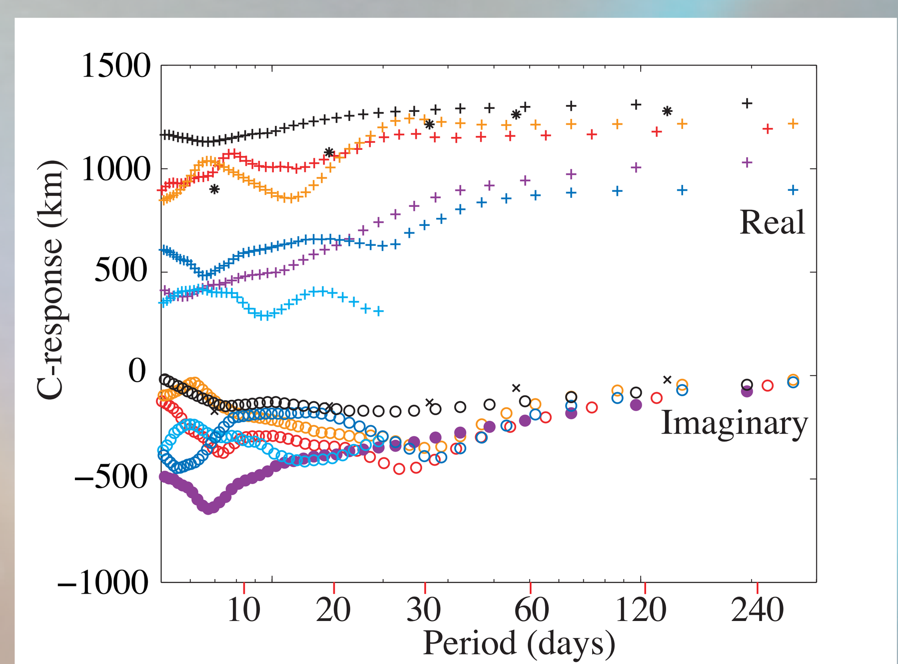

Figure 4. C estimates for different local times. Magsat values from Constable and Constable (2004) are shown in black (* and x) for comparison.

Red	0-4 hrs, 2003 (coherency > 0.6)
Orange	4-8 hrs, 2001 (coherency > 0.8)
Purple	8-12 hrs, 2002 (coherency > 0.8)
Cyan	12-16 hrs, 2003 (coherency > 0.8)
Dk Blue	16-20 hrs, 2001 (coherency > 0.6)
Black	20-24 hrs, 2002 (coherency > 0.8)

8. ELECTRICAL CONDUCTIVITY

- Figure 5A presents a preliminary electrical conductivity profile using data from local times between 4 to 8 hours (obtained using Occam (Constable et al., 1987), RMS = 3)
- A comparison between the band averaged data and the model C estimates is shown in Figure 5B

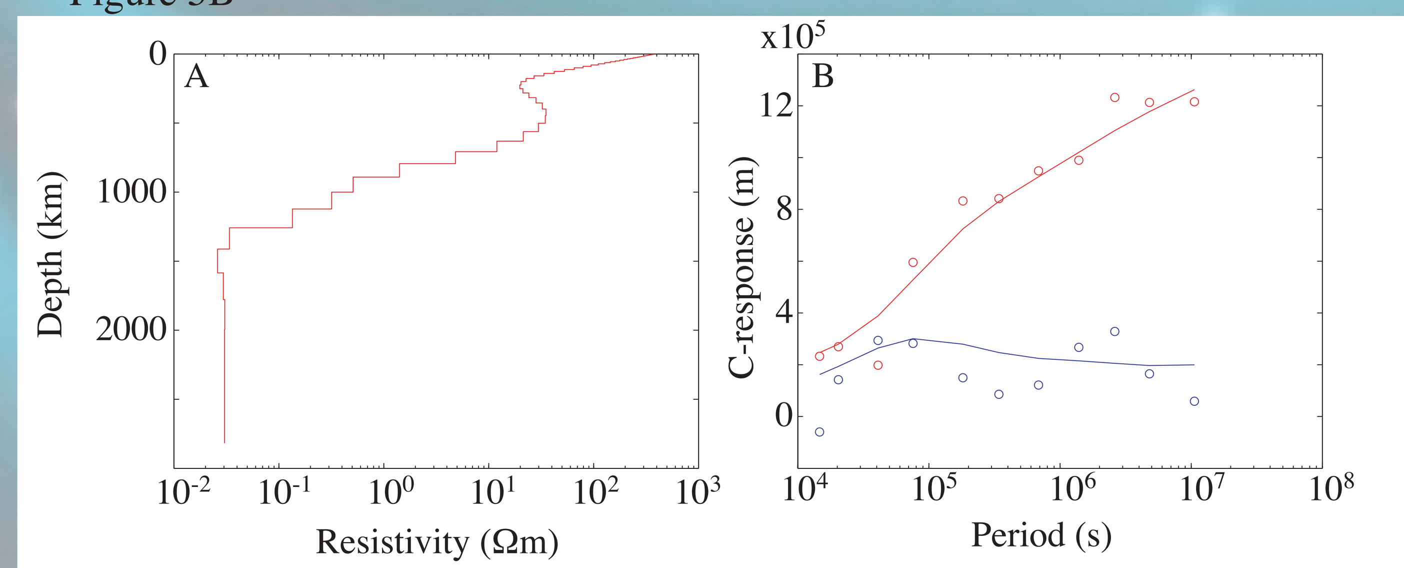

Figure 5. Preliminary results for 4-8 hours local time. 5A: Conductivity. 5B: Data (symbols) and model (lines) for the real (red) and negative imaginary (blue) parts of C.

9. FUTURE WORK

- C estimates for passes from 2004 and 2005
- Invert the local time C estimates to obtain electrical conductivity profiles for all local times
- Estimate electrical conductivity profiles for as long a timeseries as possible

10. REFERENCES

Balasis et al., 2004. Geophys. Res. Lett., doi:10.1029/2004GL020147.
Constable et al., 1987. Geophysics, 52, 289-300.
Constable and Constable, 2004. G^3, doi:10.1029/2003GC000634.
Dolginov, 1972. Geomag. Aeron., 12, 611-617.
Langel and Estes, 1985. J. Geophys. Res., 90, 2487-2494.
Olsen, 1999. Surv. Geophys., 20, 309-340.
Olsen et al., 2006. Geophys. J. Int., in press.
Sabaka et al., 2004. Geophys. J. Int., 159, 521-547.

UCSD

IGPP